Functional Characterization of Tet-AMPA [Tetrazolyl-2-amino-3-(3-hydroxy-5-methyl-4-isoxazolyl)propionic Acid] Analogues at Ionotropic Glutamate Receptors GluR1−GluR4. The Molecular Basis for the Functional Selectivity Profile of 2-Bn-Tet-AMPA

Anders A. Jensen,*,† Thomas Christesen,† Ulrik Bølcho,‡ Jeremy R. Greenwood,† Giovanna Postorino,† Stine B. Vogensen,† Tommy N. Johansen,† Jan Egebjerg,‡,§ Hans Bräuner-Osborne,† and Rasmus P. Clausen†

Department of Medicinal Chemistry, Faculty of Pharmaceutical Sciences, University of Copenhagen, Universitetsparken 2, DK-2100 Copenhagen, Denmark, Department of Molecular and Structural Biology, C. F. Møllers Allé Building 130, University of Aarhus, DK-8000 Aarhus, Denmark, and Department of Molecular Neurobiology, H. Lundbeck A/S, Ottiliavej 9, DK-2500 Valby, Denmark

Received May 7, 2007

Four 2-substituted Tet-AMPA [Tet = tetrazolyl, AMPA = 2-amino-3-(3-hydroxy-5-methyl-4-isoxazolyl)-propionic acid] analogues were characterized functionally at the homomeric AMPA receptors $GluR1_i$, $GluR2Q_i$, $GluR3_i$, and $GluR4_i$ in a Fluo-4/Ca^{2+} assay. Whereas 2-Et-Tet-AMPA, 2-Pr-Tet-AMPA, and 2-iPr-Tet-AMPA were nonselective GluR agonists, 2-Bn-Tet-AMPA exhibited a 40-fold higher potency at $GluR4_i$ than at $GluR1_i$. Examination of homology models of the S1−S2 domains of GluR1 and GluR4 containing 2-Bn-Tet-AMPA suggested four nonconserved residues in a region adjacent to the orthosteric site as possible determinants of the $GluR4_i$/$GluR1_i$ selectivity. In a mutagenesis study, doubly mutating M686V/I687A in $GluR1_i$ in combination with either D399S or E683A increased both the potency and the maximal response of 2-Bn-Tet-AMPA at this receptor to levels similar to those elicited by the agonist at $GluR4_i$. The dependence of the novel selectivity profile of 2-Bn-Tet-AMPA upon residues located outside of the orthosteric site underlines the potential for developing GluR subtype selective ligands by designing compounds with substituents that protrude beyond the (*S*)-Glu binding pocket.

Introduction

(*S*)-Glutamate [(*S*)-Glu[a]] is the major excitatory neurotransmitter in the central nervous system, where the amino acid is involved in physiological processes important for memory and learning, motor control, and neural plasticity and development.[1−3] On the other hand, (*S*)-Glu is also a key mediator of the neurotoxic processes connected with stroke and ischemia, just as excessive glutamatergic signaling appears to constitute a major component in neurodegenerative disorders such as Parkinson's disease, Alzheimer's disease, and amyotrophic lateral sclerosis. Intervention in glutamatergic neurotransmission has also been proposed to be beneficial in the treatment of epilepsy, pain, and certain psychiatric disorders.[1,4]

(*S*)-Glu exerts its physiological effects through two receptor classes, the metabotropic and ionotropic glutamate receptors (mGluRs and iGluRs, respectively).[1,2,5] The eight mGluRs mediate metabolic intracellular responses to (*S*)-Glu via coupling to various G-proteins and second messenger cascades, whereas the iGluRs are ligand-gated ion channels that mediate the fast synaptic response to extracellular (*S*)-Glu. The iGluR is a homo- or heteromeric receptor complex assembled from four subunits, and each iGluR subunit consists of a large extracellular N-terminal domain sharing weak amino acid sequence homology with bacterial periplasmic binding proteins; the extracellular S1 and S2 domains, which also exhibit sequence homology with bacterial periplasmic binding proteins and comprise the orthosteric site of the receptor; and a transmembrane domain comprised of the transmembrane regions M1, M3, and M4 and the re-entrant loop, M2. The M2 loops of the four subunits in the assembled iGluR tetramer form an ion pore through which the cations Na^+ and Ca^{2+} enter the cell upon receptor activation by agonist binding to the S1−S2 domain.[1,2,6]

The 18 iGluR subunits cloned to date are divided into seven *N*-methyl-D-aspartic acid (NMDA), four 2-amino-3-(3-hydroxy-5-methyl-4-isoxazolyl)propionic acid (AMPA), and five kainate receptor subunits based on their respective selectivities for the three agonists, as well as two orphan subunits $\delta 1$ and $\delta 2$.[1,2] The classification of the subunits into subgroups also reflects varying degrees of homology between the amino acid sequences of the receptors and differences in their signaling characteristics. The four cloned AMPA receptor subunits are termed GluR1−GluR4, and they all exist in "flip" and "flop" splice variants (termed $GluR1_i$−$GluR4_i$ and $GluR1_o$−$GluR4_o$, respectively) characterized by different desensitization kinetics and steady-state responses.[1,2,6] Furthermore, the AMPA receptor subunits are subject to RNA editing at different sites, the most notable of these being the Q/R-site located in M2 of GluR2.[1,2]

The native AMPA receptor population consists of predominantly heteromeric receptors, and this molecular heterogeneity contributes to the complexity of in vivo signaling by these receptors. Delineating the physiological roles of the respective AMPA receptor subtypes has been severely hampered over the years by a lack of subtype-selective ligands. The lack of such ligands can be ascribed to the high conservation of the orthosteric sites of the four GluR subunits, since the only residue

* Corresponding author. Phone: +45 3533 6491. Fax:+45 3533 6040. E-mail: aaj@farma.ku.dk.
† University of Copenhagen.
‡ University of Aarhus.
§ H. Lundbeck A/S.

[a] Abbreviations: AMPA, 2-amino-3-(3-hydroxy-5-methyl-4-isoxazolyl)-propionic acid; 2-Bn-Tet-AMPA, (*RS*)-2-amino-3-[3-hydroxy-5-(2-benzyl-2*H*-5-tetrazolyl)-4-isoxazolyl]propionic acid; 2-Et-Tet-AMPA, (*RS*)-2-amino-3-[3-hydroxy-5-(2-ethyl-2*H*-5-tetrazolyl)-4-isoxazolyl]propionic acid; 2-Pr-Tet-AMPA, (*RS*)-2-amino-3-[3-hydroxy-5-(2-propyl-2*H*-5-tetrazolyl)-4-isoxazolyl]propionic acid; 2-iPr-Tet-AMPA, (*RS*)-2-amino-3-[3-hydroxy-5-(2-isopropyl-2*H*-5-tetrazolyl)-4-isoxazolyl]propionic acid; 1-Me-Tet-AMPA, (*RS*)-2-amino-3-[3-hydroxy-5-(1-methyl-2*H*-5-tetrazolyl)-4-isoxazolyl]propionic acid; CTZ, cyclothiazide; (*S*)-Glu, (*S*)-glutamate; HEK293, human embryonic kidney 293; iGluR, ionotropic glutamate receptor; mGluR, metabotropic glutamate receptor; MM-GBSA, molecular mechanics-generalized born surface area; NMDA, *N*-methyl-D-aspartic acid; Tet-AMPA, tetrazolyl-AMPA; WT, wild type.

10.1021/jm070532r CCC: $37.00
Published on Web 08/02/2007

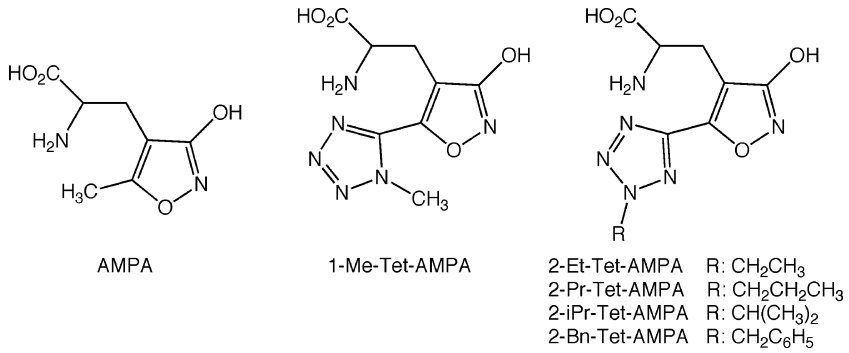

Figure 1. Chemical structures of AMPA and the Tet-AMPA analogues (racemic mixtures) characterized in this study.

differing between the orthosteric sites of the four subunits is a tyrosine residue in GluR1 and GluR2 (Tyr^{702} in GluR2), corresponding to a phenylalanine residue in GluR3 and GluR4.[6] AMPA agonists such as Cl-HIBO, (*S*)-CW-399, and (*R*,*S*)-2-amino-3-(3-hydroxy-pyridiazin-4-yl 1-oxide)propionic acid display significant preferences for the GluR1 and GluR2 subtypes over the GluR3 and GluR4 subtypes, and the subgroup selectivity of these agonists has been attributed to the Tyr/Phe switch between these receptors.[7−9] However, to date no agonist truly selective for one AMPA receptor subtype has been published.

In two recent studies, we have reported the design and synthesis of a series of four 2-substituted tetrazolyl-AMPA (Tet-AMPA) analogues [(*RS*)-2-amino-3-[3-hydroxy-5-(2-ethyl-2*H*-5-tetrazolyl)-4-isoxazolyl]propionic acid (2-Et-Tet-AMPA), (*RS*)-2-amino-3-[3-hydroxy-5-(2-propyl-2*H*-5-tetrazolyl)-4-isoxazolyl]propionic acid (2-Pr-Tet-AMPA), (*RS*)-2-amino-3-[3-hydroxy-5-(2-isopropyl-2*H*-5-tetrazolyl)-4-isoxazolyl]-propionic acid (2-iPr-Tet-AMPA) and (*RS*)-2-amino-3-[3-hydroxy-5-(2-benzyl-2*H*-5-tetrazolyl)-4-isoxazolyl]propionic acid (2-Bn-Tet-AMPA), Figure 1] and their binding characteristics at native AMPA, KA, and NMDA receptors as well as recombinant homomeric AMPA receptor subtypes $GluR1_o$−$GluR4_o$.[10,11] The affinity rank order of three 2-alkyl-Tet-AMPA analogues at $GluR1_o$−$GluR4_o$ was found to be 2-Et-Tet-AMPA > 2-Pr-Tet-AMPA > 2-iPr-Tet-AMPA with at least 10-fold difference between 2-Et-Tet-AMPA and 2-Pr-Tet-AMPA and between 2-Pr-Tet-AMPA and 2-iPr-Tet-AMPA at all four receptor subtypes.[11] Neither 2-Et-Tet-AMPA, 2-Pr-Tet-AMPA, nor 2-iPr-Tet-AMPA displayed a preference for a specific GluR subtype, as their respective K_i values only differed 3−7-fold among the $GluR1_o$–$GluR4_o$ subtypes. By contrast, the benzyl analogue 2-Bn-Tet-AMPA exhibited a K_i value of 200 nM at $GluR4_o$ and 2-, 4-, and 40-fold higher K_i values at $GluR3_o$, $GluR2_o$, and $GluR1_o$, respectively, thus being able to differentiate non-$GluR1_o$ AMPA receptors from $GluR1_o$ in terms of binding affinity.[11] In the present work, we characterize the functional pharmacology of selected 2-substituted Tet-AMPA analogues at the rat homomeric AMPA receptor subtypes $GluR1_i$, $GluR2Q_i$, $GluR3_i$, and $GluR4_i$ and investigate the molecular basis for the functional selectivity profile of 2-Bn-Tet-AMPA.

Results

Functional Characterization of Tet-AMPA Analogues at the Stable GluR-HEK293 Cell Lines. The functional properties of the 2-substituted Tet-AMPA analogues 2-Et-Tet-AMPA, 2-Pr-Tet-AMPA, 2-iPr-Tet-AMPA, and 2-Bn-Tet-AMPA were characterized at $GluR1_i$−$GluR4_i$ stably expressed in human embryonic kidney 293 (HEK293) cell lines in the Fluo-4/Ca^{2+} assay in the presence of 100 μM cyclothiazide (CTZ) to eliminate desensitization. Whereas the 2-Et-Tet-AMPA analogue was a quite potent AMPA receptor agonist, exhibiting 2−7 fold higher potencies at $GluR1_i$−$GluR4_i$ than (*S*)-Glu, introducing propyl and isopropyl substituents at the 2-position of the tetrazolyl ring led to significantly reduced agonist potencies at all four subtypes (Figure 2 and Table 1). 2-Bn-Tet-AMPA displayed similar EC_{50} values at the $GluR3_i$ and $GluR4_i$ subtypes to those of the propyl and isopropyl analogues. But unlike these two analogues, 2-Bn-Tet-AMPA displayed a significant degree of selectivity in its potencies at the four subtypes with the rank order $GluR4_i$ > $GluR3_i$ > $GluR1_i$ ≥ $GluR2Q_i$. Thus 2-Bn-Tet-AMPA exhibited approximately 40-fold higher potency at $GluR4_i$ than at $GluR1_i$ (Table 1 and Figure 3). The four 2-substituted Tet-AMPA analogues were full agonists or partial agonists at all four GluR subtypes (Figures 2 and 3 and Table 1).

Unlike the very potent agonist 2-Me-Tet-AMPA,[12,13] its 1-Me-Tet-AMPA isomer (*RS*)-2-amino-3-[3-hydroxy-5-(1-methyl-2*H*-5-tetrazolyl)-4-isoxazolyl]propionic acid was found to be completely inactive at $GluR1_i$ and $GluR2Q_i$ in concentrations up to 3 mM both as an agonist and as an antagonist. At the $GluR3_i$- and $GluR4_i$-HEK 293 cell lines, 1-Me-Tet-AMPA elicited agonist responses at concentrations of 1 mM and above (Table 1 and Figure 2). However, it may not necessarily be 1-Me-Tet-AMPA itself that is eliciting these agonist responses. Considering the synthetic route used for the preparation of 1-Me-Tet-AMPA, it is not unlikely that the compound sample could contain trace concentrations of 2-Me-Tet-AMPA. Since (*S*)-2-Me-Tet-AMPA has exhibited nanomolar EC_{50} values at $GluR3_o$ and $GluR4_o$ expressed in *Xenopus* oocytes,[13] trace concentrations (0.01−0.1%) of this compound in the 1-Me-Tet-AMPA sample could give rise to the observed activities at $GluR3_i$ and $GluR4_i$.

Investigation of the Binding Mode and Energies of 2-Bn-Tet-AMPA to GluRs. The binding mode of (*S*)-2-Bn-Tet-AMPA to various GluR subtypes was examined using the recently published GluR2-S1S2J/(*S*)-2-Bn-Tet-AMPA crystal structure[11] and homology models of the GluR1- and GluR4-S1S2 domains based on this crystal structure (Figure 4). In the GluR2-S1S2J/(*S*)-2-Bn-Tet-AMPA crystal structure we identified the four residues, Ser^{403}, Ala^{687}, Val^{690}, and Ala^{691}, located at the shortest distance from the benzyl group of 2-Bn-Tet-AMPA, and also they differed from the GluR1, where they correspond to the residues Asp^{399}, Glu^{683}, Met^{686}, and Ile^{687}, respectively. The four residues are conserved in GluR2, GluR3, and GluR4 (Figure 4A). According to the GluR2-S1S2J/(*S*)-2-Bn-Tet-AMPA crystal structure and the GluR1-S1S2 homology model based on this structure, these four residues appear to be situated at considerable distances from the benzyl group of (*S*)-2-Bn-Tet-AMPA. In the GluR1-S1S2 homology model, the distances are as follows: 3 Å (Asp^{399}), 8 Å (Glu^{683}), 9 Å (Met^{686}), and 12 Å (Ile^{687}). Nevertheless, these are the residues closest to the benzyl group of (*S*)-2-Bn-Tet-AMPA that are not

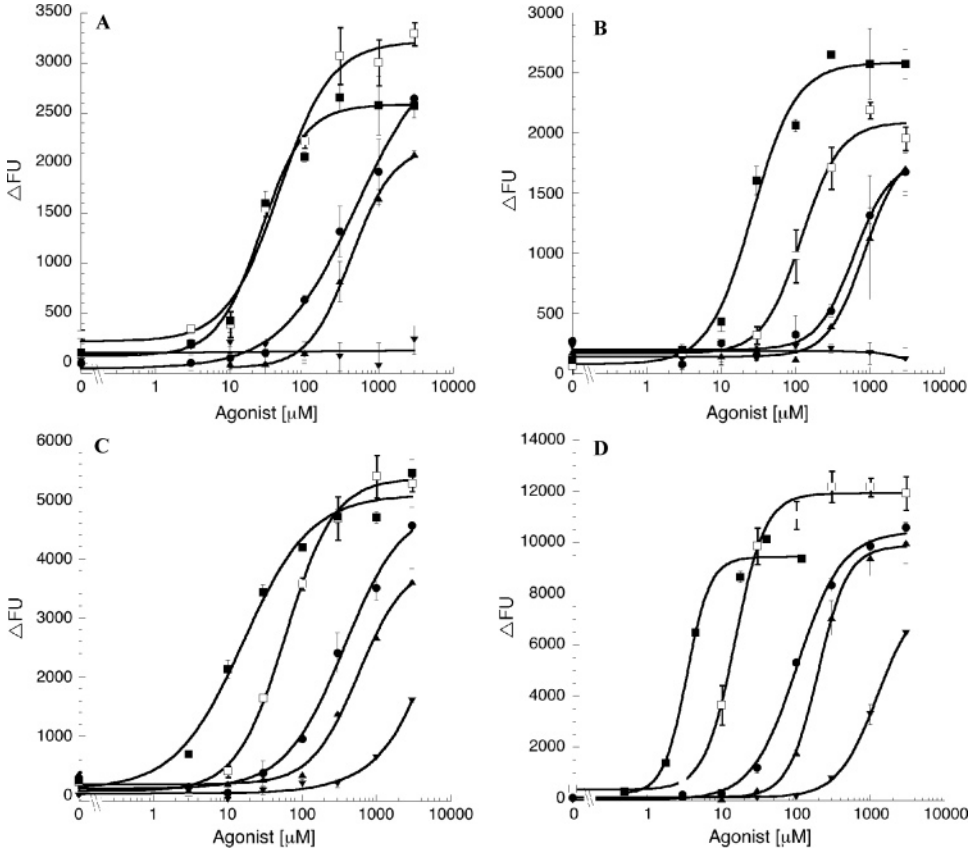

Figure 2. Functional profiles of (*S*)-Glu and alkyl-Tet-AMPA analogues at recombinant AMPA receptors in the Fluo-4/Ca^{2+} assay. Concentration−response curves for (*S*)-Glu (□), 2-Et-Tet-AMPA (■), 2-Pr-Tet-AMPA (●), 2-iPr-Tet-AMPA (▲), and 1-Me-Tet-AMPA (▼) at homomeric rat AMPA receptors $GluR1_i$ (A), $GluR2Q_i$ (B), $GluR3_i$ (C), and $GluR4_i$ (D) stably expressed in HEK293 cells were obtained in the presence of 100 μM CTZ. The response is given as change in fluorescence units (△FU) upon application of agonist to the cells. Data are means ± SD of triplicate determinations of single representative experiments.

Table 1. Functional Characteristics of (*S*)-Glu and Five Tet-AMPA Analogues at the Stable $GluR1_i$-, $GluR2Q_i$-, $GluR3_i$-, and $GluR4_i$-HEK293 Cell Lines in the Ca^{2+}/Fluo-4 Assay[a]

	$GluR1_i$		$GluR2Q_i$		$GluR3_i$		$GluR4_i$	
compd	EC_{50} [pEC_{50} ± SEM]	R_{max} ± SEM	EC_{50} [pEC_{50} ± SEM]	R_{max} ± SEM	EC_{50} [pEC_{50} ± SEM]	R_{max} ± SEM	EC_{50} [pEC_{50} ± SEM]	R_{max} ± SEM
(*S*)-Glu	71 [4.2 ± 0.10]	-	140 [3.9 ± 0.03]	-	67 [4.2 ± 0.04]	-	28 [4.6 ± 0.08]	-
2-Et-Tet-AMPA	42 [4.4 ± 0.08]	83 ± 6	52 [4.3 ± 0.04]	94 ± 8	18 [4.8 ± 0.04]	95 ± 2	4.0 [5.4 ± 0.06]	94 ± 4
2-Pr-Tet-AMPA	480[b] [3.3 ± 0.06]	82 ± 3[b]	830 [3.1 ± 0.16]	89 ± 3[b]	450[b] [3.4 ± 0.07]	85 ± 3[b]	79 [4.2 ± 0.19]	97 ± 5
2-iPr-Tet-AMPA	550[b] [3.3 ± 0.07]	73 ± 3[b]	~1000[c] [~3]	73 ± 5[c]	~700[c] [3.2 ± 0.09]	73 ± 3[c]	160[b] [3.8 ± 0.13]	83 ± 7[b]
2-Bn-Tet-AMPA	~3000[c] [<2.5]	42 ± 3[c]	>3000[c] [<2.5]	19 ± 2[c]	~1000[c] [~3]	58 ± 6[c]	75 [4.2 ± 0.14]	113 ± 6
1-Me-Tet-AMPA	>3000 [<2.5]	NR[d]	>3000 [<2.5]	NR	>3000[c] [<2.5]	22 ± 3[c]	~3000[c] [<2.5]	79 ± 7[c]

[a] The EC_{50} values of the agonists are given in μM (with pEC_{50} ± SEM values in brackets), and the R_{max} values are given as maximal responses elicited by the Tet-AMPA analogues in percent of R_{max} of (*S*)-Glu at the respective GluRs, unless otherwise indicated. [b] The concentration−response curves for 2-Pr-Tet-AMPA and 2-iPr-Tet-AMPA at the indicated receptors had not reach saturation levels completely, so the EC_{50} and R_{max} values are determined on the basis of the curve fits of the data. [c] The concentration−response curves for 2-iPr-Tet-AMPA, 2-Bn-Tet-AMPA, and 1-Me-Tet-AMPA at the indicated receptors did not reach saturation levels, so the EC_{50} values are estimates and R_{max} values are given as the response elicited by 3 mM of the agonists in percent of the R_{max} for (*S*)-Glu. [d] NR, no significant response was observed for 3 mM 1-Me-Tet-AMPA.

conserved throughout the four GluR subtypes (Figure 4A). In addition, these residues are fairly close to the flexible side chain of Met^{708}, the conformation of which is known to be ligand dependent, the distances being 5, 5, 5, and 8 Å for Asp^{399}, Glu^{683}, Met^{686}, and Ile^{687}, respectively.[11,14]

As previously described, redocking to the experimental complex of (*S*)-2-Bn-Tet-AMPA with GluR2-S1S2J and a GluR1 homology model derived from it, followed by molecular mechanics-generalized born surface area (MM-GBSA) binding energy calculations, gave reasonably good agreement with the observed GluR1:GluR2 binding selectivity.[11] In order to further examine the links between structure and function, we extended this approach to all four WT GluRs and the GluR1 mutants under investigation. The estimated binding energies according to MM-GBSA at a degree of binding domain closure approximating that of the experimental GluR2:(*S*)-2-Bn-Tet-AMPA complex are given in Table 2 and clearly show the strong preference of (*S*)-2-Bn-Tet-AMPA for GluR4 over GluR1 but

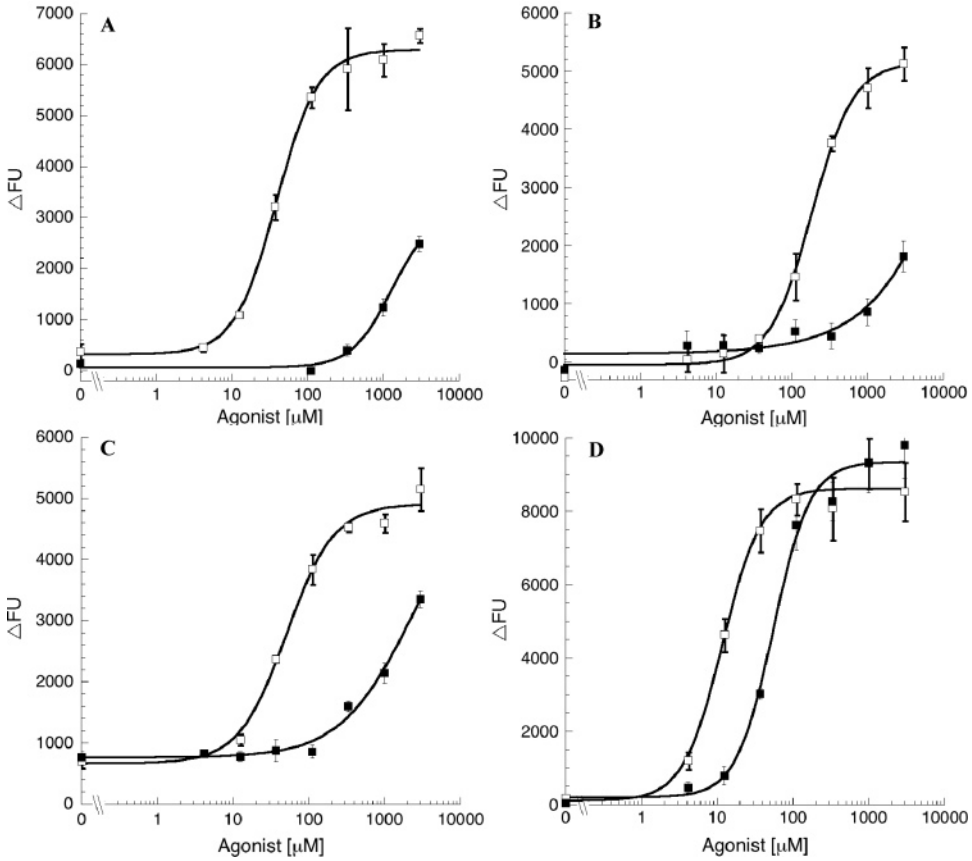

Figure 3. Functional profiles of 2-Bn-Tet-AMPA at recombinant AMPA receptors in the Fluo-4/Ca^{2+} assay. The concentration−response curves for (*S*)-Glu (□) and 2-Bn-Tet-AMPA (■) at homomeric rat AMPA receptors $GluR1_i$ (A), $GluR2Q_i$ (B), $GluR3_i$ (C), and $GluR4_i$ (D) stably expressed in HEK293 cells were obtained in the presence of 100 μM CTZ. The response is given as change in fluorescence units (△FU) upon application of agonist to the cells. Data are means ± SD of triplicate determinations of single representative experiments.

a lesser selectivity vs GluR2 and negligibly weaker binding energy at GluR3, in agreement with the binding data.[11]

Functional Characterization of 2-Bn-Tet-AMPA at WT and Mutant GluRs. To elucidate the molecular origin of the selectivity profile of 2-Bn-Tet-AMPA, the four residues identified in the docking experiments were subjected to a mutagenesis study. We attempted here to reintroduce "$GluR4_i$-like" potency for 2-Bn-Tet-AMPA into $GluR1_i$ via mutations of the four residues in $GluR1_i$ identified as possible selectivity determinants to the corresponding residues in $GluR4_i$ (Figure 4C,D).

HEK293 cells expressing WT $GluR1_i$, WT $GluR4_i$, and mutant $GluR1_i$ receptors were constructed via transfection with the respective cDNAs and subsequent antibiotic selection of the transfected cells with G418 for 2−3 weeks (to kill untransfected cells in the cell population), after which the agonist responses of (*S*)-Glu and 2-Bn-Tet-AMPA at the various polyclonal cell lines were determined using the Fluo-4/Ca^{2+} assay in the presence of 100 μM CTZ. The concentration−response curves displayed by 2-Bn-Tet-AMPA at the polyclonal WT $GluR1_i$- and WT $GluR4_i$-expressing HEK293 cells lines were significantly right-shifted compared to those obtained at the stable "monoclonal" $GluR1_i$- and $GluR4_i$-HEK293 cell lines, whereas the potencies obtained for (*S*)-Glu at the monoclonal and polyclonal cell lines were fairly similar (Tables 1 and 3). Analogously to the 2-Bn-Tet-AMPA profile at the stable monoclonal GluR cell lines, 2-Bn-Tet-AMPA displayed >10 fold higher potency at WT $GluR4_i$ than at WT $GluR1_i$, where the agonist elicited a barely detectable signal at concentrations up to 3 mM (Table 3 and Figure 5A). Considering the relatively low agonist responses obtained in the Ca^{2+}/Fluo-4 assay using polyclonal cell lines, the potencies and efficacies obtained for (*S*)-Glu and 2-Bn-Tet-AMPA at these WT and mutant GluRs cannot be considered accurate data. Thus, the data presented in Table 3 was only used as a rough guidance in the search for the residues determining the selectivity profile of 2-Bn-Tet-AMPA, and the importance of the identified residues was subsequently verified at GluRs expressed in *Xenopus* oocytes (see later).

In this mutagenesis study, all but two $GluR1_i$ mutants exhibited functional characteristics for (*S*)-Glu similar to that displayed by WT $GluR1_i$ (Table 3). By contrast, the low potencies of 2-Bn-Tet-AMPA at WT and mutant $GluR1_i$ expressing cells made it impossible to determine accurate EC_{50} and R_{max} values at these receptors. However, the response size elicited by 3 mM 2-Bn-Tet-AMPA at the respective mutant receptors relative to the responses measured at cells expressing WT $GluR1_i$ and WT $GluR4_i$ allowed us to estimate whether or not the introduction of a given mutation in $GluR1_i$ had increased the agonist activity of 2-Bn-Tet-AMPA toward a "$GluR4_i$-like" response (Table 3 and Figure 5B).

The three $GluR1_i$ single-mutants E683A, M686V, and I687A exhibited responses to 2-Bn-Tet-AMPA not significantly different from that of WT $GluR1_i$. 2-Bn-Tet-AMPA was able to elicit small responses at concentrations of 1 mM and above in cells expressing the fourth single-mutant D399S-$GluR1_i$, indicating some gain of agonist activity (Figure 5B and Table 3). The functional characteristics of 2-Bn-Tet-AMPA at the two $GluR1_i$ double-mutants D399S/E683A and M686V/I687A differed significantly from that of the WT receptor. Neither 2-Bn-Tet-AMPA nor (*S*)-Glu evoked measurable responses in "polyclonal" HEK293 cells expressing the D399S/E683A-$GluR1_i$ mutant at concentrations up to 3 mM (data not shown), which

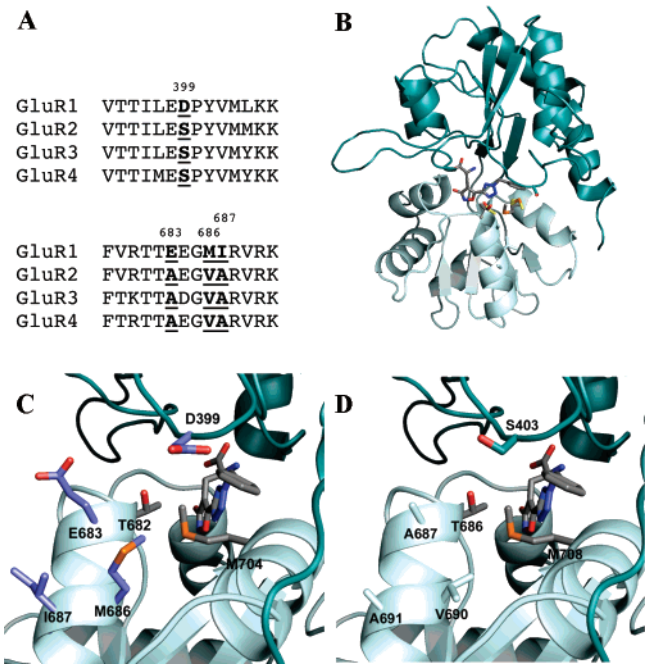

Figure 4. Binding mode of (*S*)-2-Bn-Tet-AMPA to AMPA receptors. (A) Alignment of two regions of rat AMPA receptors GluR1−4 and identification of the four residues located near the benzyl ring of (*S*)-2-Bn-Tet-AMPA conserved in GluR2−4 but not in GluR1. The numbering of the four residues in GluR1 is indicated above the residues. (B) The GluR2-S1S2J/(*S*)-2-Bn-Tet-AMPA crystal structure. (C) Binding mode of (*S*)-2-Bn-Tet-AMPA in a homology model of GluR1-S1S2 domain based on the GluR2-S1S2J/(*S*)-2-Bn-Tet-AMPA crystal structure. (D) Binding mode of (*S*)-2-Bn-Tet-AMPA in a homology model of GluR4-S1S2 domain based on the GluR2-S1S2J/(*S*)-2-Bn-Tet-AMPA crystal structure.

Table 2. Binding Energies of 2-Bn-Tet-AMPA to Models of WT GluR1, WT GluR2, WT GluR3, WT GluR4, and Mutant GluR1 S1−S2J Domains, Estimated by MM-GBSA

Receptor model	MM-GBSA binding energy (kcal/mol)
WT GluR4	−54.89
WT GluR3	−54.52
GluR1-E683A/M686V/I687A	−53.48
WT GluR2	−53.33
GluR1-D399S/E683A/M686V/I687A	−53.32
GluR1-D399S/E683A	−51.85
GluR1-E683A	−51.70
GluR1-D399S/M686V/I687A	−51.40
GluR1-M686V/I687A	−50.63
GluR1-I687A	−50.49
GluR1-D399S	−50.08
WT GluR1	−49.39
GluR1-M686V	−49.11

is notable considering that neither the D399S nor the E683A mutant appeared to be functionally impaired. On the other hand, 2-Bn-Tet-AMPA displayed a significantly left-shifted concentration−response curve at M686V/I687A-GluR1$_i$ compared to WT GluR1$_i$ (Figure 5B). The addition of either D399S or E683A, yielding the GluR1$_i$ mutants D399S/M686V/I687A and E683A/M686V/I687A, further increased the efficacy displayed by 2-Bn-Tet-AMPA to levels comparable to that observed at WT GluR4$_i$ (Figure 5B and Table 3). The relative efficacy of 2-Bn-Tet-AMPA compared to the maximal response of (*S*)-Glu was similar in cells expressing WT GluR4$_i$ and the two triple-mutants, and the estimated potencies displayed by the agonist at the three receptors were also comparable (Table 3 and Figure 5A). The quadruple GluR1$_i$ mutant D399S/E683A/M686V/I687A was virtually nonresponsive to 2-Bn-Tet-AMPA and (*S*)-Glu at concentrations up to 3 mM, which was not surprising considering the functional impairment of the D399S/E683A-GluR1$_i$ mutant (data not shown).

Functional Characterization of 2-Bn-Tet-AMPA at GluRs Expressed in *Xenopus* oocytes. In order to confirm the potency and maximal response determinations for 2-Bn-Tet-AMPA from the studies with stable and polyclonal HEK293 expressing GluRs, we studied the functional pharmacology of the agonist at WT GluR1$_i$, WT GluR4$_i$, and the D399S/M686V/I687A-GluR1$_i$ mutant expressed in *Xenopus* oocytes. The efficacies of 2-Bn-Tet-AMPA and (*S*)-Glu were recorded in the presence of 100 μM CTZ. The agonist responses elicited by 2-Bn-Tet-AMPA at WT GluR4$_i$ and D399S/M686V/I687A-GluR1$_i$ had almost reached saturation levels at a 3 mM concentration. Thus, on the basis of the fitted concentration−response curves, it was possible to estimate the EC_{50} values and maximal responses (in percent of the maximal response of (*S*)-Glu) for 2-Bn-Tet-AMPA at these two receptors. 2-Bn-Tet-AMPA was found to be a partial agonist at WT GluR4$_i$, displaying an EC_{50} value of 490 μM (pEC_{50} = 3.31 ± 0.03) and a maximal response of 63% (±6%) of that of (*S*)-Glu. By contrast, the agonist was a significantly weaker agonist at WT GluR1$_i$, where the concentration−response curve did not reach saturation levels at concentrations up to 3 mM (Figure 6). Introducing the triple mutation D399S/M686V/I687A into GluR1$_i$ gave rise to an agonist response to 2-Bn-Tet-AMPA very similar to that elicited at WT GluR4$_i$, as 2-Bn-Tet-AMPA displayed an EC_{50} value of 580 μM (pEC_{50} = 3.24 ± 0.09) and a maximal response of 60% (±6%) of that of (*S*)-Glu (Figure 6).

Discussion

In the present study we have characterized the functional pharmacology of a series of Tet-AMPA analogues at the rat AMPA receptors GluR1$_i$−GluR4$_i$; as in a previous study, these compounds had presented interesting binding characteristics at the flop variants of the receptors.[11] The rank orders of agonist potencies for the 2-alkyl-Tet-AMPA analogues were 2-Et-Tet-AMPA > 2-Pr-Tet-AMPA ≥ 2-iPr-Tet-AMPA at all the GluR subtypes, which is in good agreement with the previous binding study, although the differences in EC_{50} values between the agonists were considerably smaller than the differences in their binding affinities.[11] Thus, 2-Et-Tet-AMPA retained much of the potency of 2-Me-Tet-AMPA, the most potent AMPA receptor agonist reported to date,[12,13] whereas the larger propyl and isopropyl substituents at the 2-position of the tetrazole ring were clearly unfavorable for agonist activity. Interestingly, 2-Pr-Tet-AMPA and 2-iPr-Tet-AMPA displayed similar agonist potencies at the flip variants of the GluRs, although the former compound has displayed 15−30-fold higher binding affinities at GluR1$_o$−GluR4$_o$ than 2-iPr-Tet-AMPA (Table 1).[11] The EC_{50} values for 2-Et-Tet-AMPA, 2-Pr-Tet-AMPA, and 2-iPr-Tet-AMPA varied 13-, 12-, and 4-fold across the four GluR subtypes, and 2-Bn-Tet-AMPA displayed an EC_{50} value of 75 μM at GluR4$_i$ and 13-, 40-, and >40-fold higher EC_{50} values at GluR3$_i$, GluR1$_i$, and GluR2Q$_i$, respectively (Table 1). Finally, the introduction of even a small substituent, a methyl group, at the 1-position of the tetrazolyl ring has a detrimental effect on the agonist potency of the compound (Figure 2).

The EC_{50} value determined for 2-Bn-Tet-AMPA at GluR4$_i$ expressed in oocytes was 6-fold higher than at GluR4$_i$ expressing monoclonal cells in the Ca^{2+}/Fluo-4 assay (Table 2 and Figure 6). Furthermore, in contrast to the full agonism displayed by 2-Bn-Tet-AMPA at GluR4$_i$ in the Ca^{2+}/Fluo-4 assay, the agonist displayed efficacy of 63% at the receptor in oocytes and has

Table 3. Functional Properties of (*S*)-Glu and 2-Bn-Tet-AMPA at Polyclonal HEK293 Cells Expressing WT $GluR1_i$, WT $GluR4_i$, and $GluR1_i$ Mutants in the Fluo-4/Ca^{2+} Assay[a]

	(*S*)-Glu	2-Bn-Tet-AMPA		
	EC_{50} (μM) [$pEC_{50} \pm$ SEM]	EC_{50} (μM) [$pEC_{50} \pm$ SEM]	R_{max} (% of $R_{max,(S)-Glu}$)	$R_{3mM}/R_{3mM\ WT\ GluR4_i}$ (%)
WT $GluR1_i$	75 [4.1 ± 0.03]	>3000	nd[c]	12 ± 3
WT $GluR4_i$	51 [4.3 ± 0.03]	435 [3.4 ± 0.04][b]	74 ± 4[b]	100
$GluR1_i$ Mutants				
D399S	69 [4.2 ± 0.05]	~3000	nd[c]	32 ± 4
E683A	39 [4.4 ± 0.06]	>3000	nd[c]	19 ± 3
M686V	63 [4.2 ± 0.04]	>3000	nd[c]	15 ± 3
I687A	140 [3.9 ± 0.05]	>3000	nd[c]	11 ± 2
D399S/E683A	nd[d]	nd[d]	nd[c]	nd[d]
M686V/I687A	76 [4.1 ± 0.04]	~500	nd[c]	54 ± 5
D399S/M686V/I687A	60 [4.2 ± 0.06]	~700	nd[c]	75 ± 5
E683A/M686V/I687A	110 [4.0 ± 0.03]	~500	nd[c]	77 ± 13
D399S/E683A/M686V/I687A	nd[d]	nd[d]	nd[c]	nd[d]

[a] EC_{50} values for (*S*)-Glu are given in μM (with $pEC_{50} \pm$ SEM values in brackets), and EC_{50} values for 2-Bn-Tet-AMPA are given as rough estimates (in μM). The $R_{3mM}/R_{3mM\ WT\ GluR4_i}$ ratios for the respective receptors are given as the response caused by 3 mM 2-Bn-Tet-AMPA at a certain receptor in percent of the response caused by 3 mM 2-Bn-Tet-AMPA at WT $GluR4_i$. [b] The concentration−response curves for 2-Bn-Tet-AMPA at WT $GluR4_i$ had not reach saturation levels completely in all experiments, so the EC_{50} and R_{max} values are determined on the basis of the curve fits of the data. [c] Not determined, as the concentration−response curves for 2-Bn-Tet-AMPA at the receptors did not reach saturation levels in concentration up to 3 mM. [d] Not determined (agonist-evoked responses were too small).

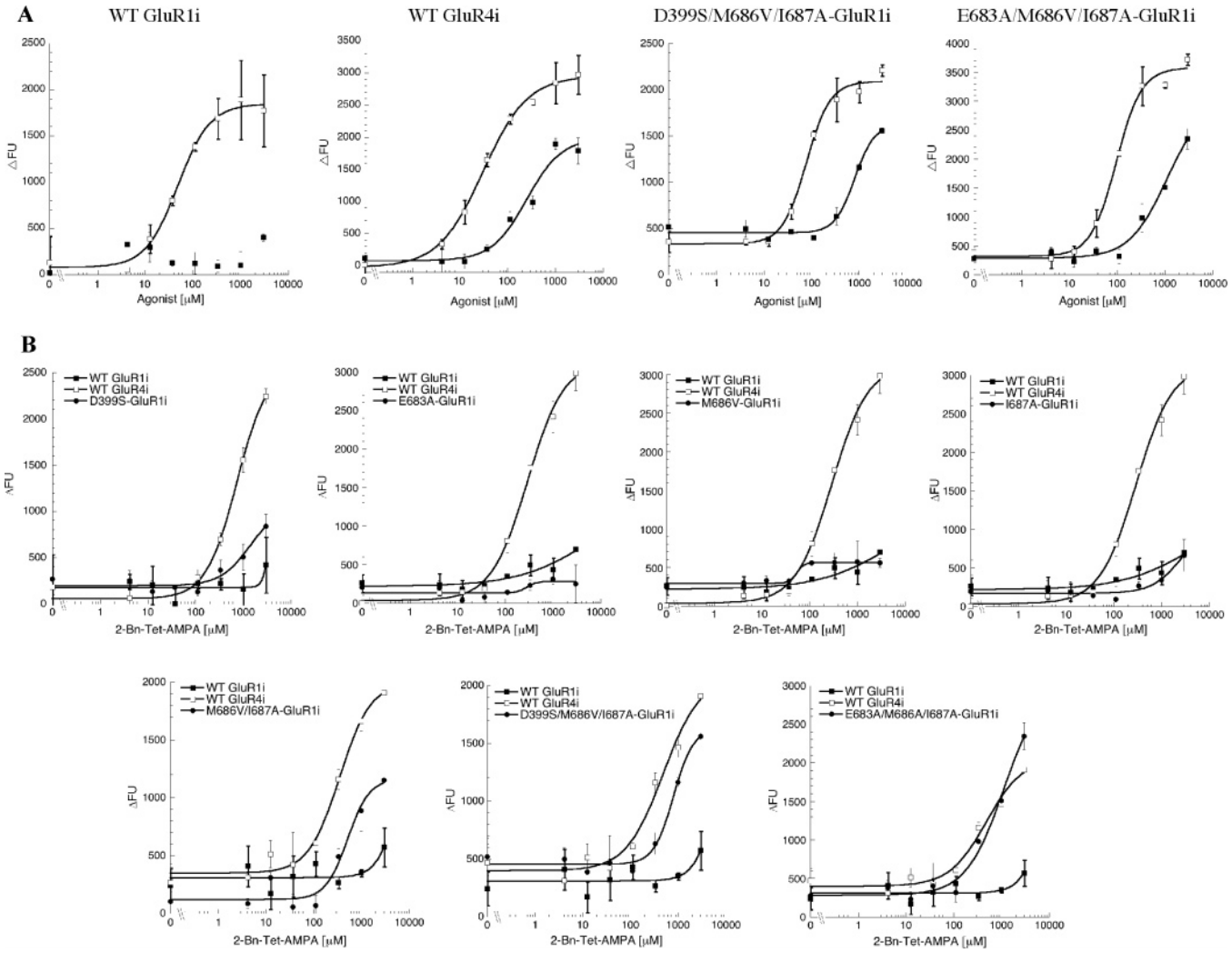

Figure 5. Functional profiles of 2-Bn-Tet-AMPA at "polyclonal" HEK293 cells expressing WT $GluR1_i$, WT $GluR4_i$, and mutant $GluR1_i$ in the Fluo-4/Ca^{2+} assay. (A) Concentration−response curves for (*S*)-Glu (□) and 2-Bn-Tet-AMPA (■) at WT $GluR1_i$, WT $GluR4_i$, and the $GluR1_i$ mutants D399S/M686V/I687A and E683A/M686V/I687A were obtained in the presence of 100 μM CTZ. (B) Concentration−response curves for 2-Bn-Tet-AMPA at WT $GluR1_i$, (■) WT $GluR4_i$ (□), and various single-, double- and triple $GluR1_i$ mutants (●) were obtained in the presence of 100 μM CTZ. The response is given as change in fluorescence units (△FU) upon application of agonist to the cells. Data are means ± SD of dublicate determinations of single representative experiments.

previously been reported to be a partial agonist with an efficacy of 84% at the non-desensitizing L483Y-mutant of $GluR2_o$ (Table 2 and Figure 6).[11] The apparent higher sensitivity of the Ca^{2+}/Fluo-4 assay could be ascribed to various differences between

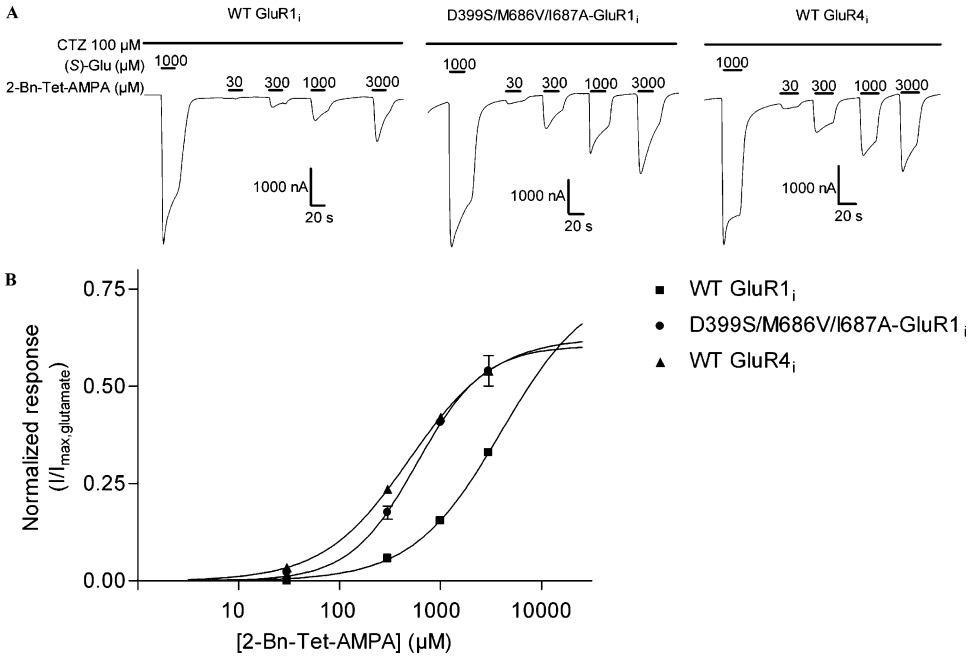

Figure 6. Functional characterization of 2-Bn-Tet-AMPA at WT and mutant GluRs expressed in *Xenopus* oocytes. (A) Traces for 2-Bn-Tet-AMPA at WT GluR1$_i$, WT GluR4$_i$, and D399S/M686V/I687A-GluR1$_i$ during a continuous application of 100 μM CTZ. The oocytes were pretreated with 100 μM CTZ for 30 s to reach maximal 2-Bn-Tet-AMPA peak current potentiation. For the 100 μM CTZ pretreated GluRs, a slow desensitization after the application of 2-Bn-Tet-AMPA is observed. (B) 2-Bn-Tet-AMPA dose−peak current response curves for 2-Bn-Tet-AMPA at WT GluR1$_i$ (■), WT GluR4$_i$ (▲), and D399S/M686V/I687A-GluR1$_i$ (●) in the presence of 100 μM CTZ, normalized to a 1000 μM (*S*)-Glu + 100 μM CTZ peak response. For each construct the data shown are from three independent experiments ($n = 3$). Data are fitted to the Hill equation.

the two assays. First, whereas the Ca^{2+}/Fluo-4 assay measures intracellular Ca^{2+} concentrations, the oocyte data represents a direct measurement of Na^+ influx through the GluR. Second, in contrast to the Ca^{2+}/Fluo-4 assay, the membrane potential is kept constant during the oocyte recordings. Third, saturation of the Fluo-4 dye with Ca^{2+} could potentially give rise to the left-shifted concentration−response curve of the agonist compared to its properties in oocytes. Finally, differences in buffer compositions and expression levels in the two assays may also account for the 6-fold difference in potencies.

The equipotency of 2-Bn-Tet-AMPA at GluR1$_i$ and GluR2Q$_i$ in the Fluo-4/Ca^{2+} assay contrasts the 10-fold difference in binding affinities displayed by the compound at GluR1$_o$ and GluR2$_o$.[11] Thus, the affinity difference for 2-Bn-Tet-AMPA between GluR2 and GluR1 does not translate into a functional difference in this assay. The fact that 2-Bn-Tet-AMPA only displays a ~6-fold lower EC_{50} value at GluR4$_i$ than at GluR1$_i$ in *Xenopus* oocytes, as opposed to the 40-fold difference in binding affinities of the compound to GluR4$_o$ vs GluR1$_o$, also seems to suggest that the 10-fold GluR2$_i$/GluR1$_i$ preference of the compound in binding might translate into a less significant functional difference (Figure 6).[11]

While it is still uncertain whether or not 2-Bn-Tet-AMPA is able to discriminate between GluR1$_i$ and GluR2Q$_i$ functionally, the agonist displays a significant GluR4$_i$/GluR1$_i$ selectivity. In the second part of this study, the molecular origin of this GluR4$_i$/GluR1$_i$ selectivity was investigated in a mutagenesis study based on the GluR2-S1S2J/(*S*)-2-Bn-Tet-AMPA crystal structure. In this structure, the glycinyl, isoxazolyl, and tetrazolyl moieties of the agonist bind to the GluR2-S1S2J in similar modes to the corresponding moieties in (*S*)-2-Me-Tet-AMPA, as per the GluR2-S1S2J/(*S*)-2-Me-Tet-AMPA crystal structure.[11,14] The phenyl group of 2-Bn-Tet-AMPA is also situated within the orthosteric site, but the group projects into an adjacent cavity in the GluR2-S1S2J, where it forms hydrophobic interactions with the residues Thr^{707}, Tyr^{711}, and Trp^{767}. Comparison of the two crystal structures reveals that the accessibility of this cavity for binding the benzyl group of 2-Bn-Tet-AMPA is the result of a regional rearrangement of three residues, Glu^{402}, Thr^{686}, and Met^{708}. The nature of the interactions between Glu^{402} and Thr^{686} that form the so-called "interdomain lock" in the S1S2 domain differ between the two crystal structures, but more importantly, the spatial reorientation of Met^{708} in the GluR2-S1S2J/(*S*)-2-Bn-Tet-AMPA structure results in the creation of an opening to this neighboring cavity, and this makes it not only possible for 2-Bn-Tet-AMPA to bind to GluRs but also to retain agonism.[11] Since these three residues, as well as all residues in this "new" cavity forming hydrophobic interactions with the benzyl group, are conserved throughout the four AMPA receptor subtypes, other residues must account for the subtype selectivity displayed by the agonist. Ser^{403} and Ala^{687}, the residues neighboring the interdomain lock residues Glu^{402} and Thr^{686}, and the residues Val^{690} and Ala^{691} located in the vicinity of Met^{708} are conserved in GluR2−4 but not in GluR1, where they correspond to Asp^{399}, Glu^{683}, Met^{686}, and Ile^{687}.

It is important to stress that the data obtained in the Ca^{2+}/Fluo-4 assay using the polyclonal cell lines expressing WT GluR1$_i$ and GluR4$_i$ and the GluR1$_i$ mutants should only be considered as crude guidance information in the search for the molecular basis for functional profile of 2-Bn-Tet-AMPA. Nevertheless, single-substitutions of any of the Asp^{399}, Glu^{683}, Met^{686}, and Ile^{687} residues in GluR1$_i$ with the corresponding GluR4 residues were clearly insufficient to convert the GluR1$_i$ response of 2-Bn-Tet-AMPA to a GluR4$_i$-like response (Table 3 and Figure 5). In view of the essential role of Met^{708} for (*S*)-2-Bn-Tet-AMPA binding in the GluR2-S1S1J structure (and due to limited quantities of 2-Bn-Tet-AMPA), we decided to focus on Met^{686} and Ile^{687}, the two nonconserved residues in proximity to the corresponding residue in GluR1, Met^{704}. Introducing the double mutation M686V/I687A in GluR1$_i$ led to a marked increase in the agonist activity of 2-Bn-Tet-AMPA (Figure 5B). On the basis of the GluR1 and GluR4 S1S2 domain homology

models, we propose that the replacement of these two residues by valine and alanine residues creates the space required for the conformational rearrangement of the Met^{704} residue to accommodate 2-Bn-Tet-AMPA binding to take place. According to the GluR1 S1S2 homology model, Met^{686} and Ile^{687} are located 6.5 and 12.8 Å from the benzyl group of 2-Bn-Tet-AMPA, respectively, with the Met^{686} residue being only 3.8 Å from Met^{704} and 4.2 Å from Ile^{687}. As can be seen from the single mutants M686V- and I687A-$GluR1_i$, it is necessary for both the Met^{686} residue and the Ile^{687} residue to be mutated in order for the activity of 2-Bn-Tet-AMPA to increase (Table 3 and Figure 5B). Thus, the presence of an alanine in position 687 with its smaller side chain than isoleucine seems to provide valine (and not methionine with its larger side chain) in position 686 the space needed for it to accommodate the conformational rearrangement of Met^{704}. Thus, we propose that these two residues are the key determinants underlying the functional selectivity displayed by 2-Bn-Tet-AMPA at $GluR1_i$ and $GluR4_i$. The further enhancement of the agonist activity of 2-Bn-Tet-AMPA observed upon addition of the D399S or the E683A mutation into M686V/I687A-$GluR1_i$ could be a reflection of an altered electronic effect of the previously negatively charged side chains of each of these two residues on the neighboring "interdomain lock" residues, Glu^{398} and Thr^{682} (corresponding to Glu^{402} and Thr^{686} in GluR2), or it could simply be a matter of having converted the structural architecture of this local region of $GluR1_i$ to be almost exactly like that in $GluR4_i$. In support of a less favorable electrostatic environment for the hydrophobic benzyl group being created by Asp^{399} and Glu^{683}, we previously described a decrease in the Coulombic reward terms for the docked ligand at GluR1, according to the scoring function.[11]

By themselves, the estimated binding energies obtained for 2-Bn-Tet-AMPA to models of the S1S2J-domains of WT GluR1−GluR14 and the various GluR1 mutants using MM-GBSA shed little light on the individual roles of the four residues (Table 2). It is important to stress that binding energies cannot be directly compared with the functional data in Tables 1 and 3, and that efficacy and domain closure, which is fixed according to the available GluR2 cocomplex, cannot be modeled by this protocol. Nevertheless, there is some qualitative correspondence between the data. For example, 2-Bn-Tet-AMPA displays a considerable difference in binding energy between WT GluR1 and WT GluR4, and furthermore, the triple mutant E683A/M686V/I687A-GluR1 regains most of the characteristics of WT GluR4 with respect to 2-Bn-Tet-AMPA, whereas the single mutants do not. On the other hand, although the energies of the two other GluR1 mutants M686V/I687A and D399S/M686V/I687A displaying a "WT GluR4-like" response to 2-Bn-Tet-AMPA also are significantly lower than that of WT GluR1, the energies of these two mutants are not lower than that of the "WT GluR1-like" E683A-GluR1 mutant (Table 2). The simplest explanation for the increased functional activity of 2-Bn-Tet-AMPA at M686V/I687A-$GluR1_i$ compared with its calculated relative binding affinity at the degree of domain closure present in the experimental GluR2-S1S2J structure is that the steric effects of Met^{686} and Ile^{687} in WT GluR1 prevent the domains from closing as tightly around the ligand. In particular, the closer movement of the helix in domain 2 containing Met^{686} and Ile^{687} toward domain 1 is sterically hindered by the side chain of Met^{704} in the presence of 2-Bn-Tet-AMPA, whereas it is not in the presence of (*S*)-Glu, and small changes in domain closure have been repeatedly associated with considerable shifts in efficacy.[9] While not easily modeled, this hypothesis could be examined by cocrystallizing the corresponding GluR1-like mutants of GluR2-S1S2J, but this is beyond the scope of the present work.

Conclusion

The functional properties exhibited by the four Tet-AMPA analogues 2-Et-Tet-AMPA, 2-Pr-Tet-AMPA, 2-iPr-Tet-AMPA, and 2-Bn-Tet-AMPA at $GluR1_i$−$GluR4_i$ were found to be in reasonable concordance with their binding characteristics at $GluR1_o$−$GluR4_o$. A couple of residues located at considerable distances from 2-Bn-Tet-AMPA in a cavity adjacent to the orthosteric site were identified as the primary molecular determinants of this selectivity. Thus, the interesting pharmacological profile of 2-Bn-Tet-AMPA arises from its ability to project out of the highly conserved orthosteric site, thereby reaching receptor regions less conserved. The observed differences in the binding modes between 2-Me-Tet-AMPA and 2-Bn-Tet-AMPA strongly underline the fact that, although the GluR-S1S2J crystal structures have revolutionized the GluR field in many ways, the bilobular S1S2 domain is still a highly flexible protein, and in the absence of reliable means of modeling this flexibility, predictions of the binding modes and pharmacological properties of future ligands based on GluR-S1S2J crystal structures complexed with existing ones will remain just that, predictions. Thus, it will be interesting to see whether future 2-substituted Tet-AMPA analogues with larger 2-substituents than 2-Bn-Tet-AMPA will turn out to be more selective GluR agonists without concomitantly reduced potencies or at what point the ligands in this series will start to become competitive antagonists or simply inactive. Furthermore, other scaffolds than Tet-AMPA may provide agonists with interesting GluR subtype selectivities when augmented with substituents reaching this neighboring cavity. Finally, in view of the interesting selectivity profile displayed by 2-Bn-Tet-AMPA at non-desensitizing GluRs, it would be highly interesting to characterize the agonist at recombinant GluRs in the absence of CTZ and at the native population of heteromeric GluR complexes.

Experimental Procedures

Materials. Culture media, serum, antibiotics, and buffers for cell culture were obtained from Invitrogen (Paisley, UK). (*S*)-Glu was purchased from Sigma (St. Louis, MO), whereas CTZ was obtained from Tocris Cookson (Bristol, UK). The construction of stable HEK293 cell lines expressing the rat homomeric AMPA receptor subtypes $GluR1_i$, $GluR2Q_i$, $GluR3_i$, and $GluR4_i$ and the synthesis of 1-Me-Tet-AMPA and the 2-substituted Tet-AMPA analogues investigated in this study have been described previously.[10,11,15] The Tet-AMPA analogues characterized pharmacologically at the GluRs in this study are all racemic mixtures.

Molecular Biology. The subcloning of rat $GluR1_i$ and rat $GluR4_i$ cDNAs from their original vectors into pcDNA3.1 has been described previously.[15] All mutant $GluR1_i$-pcDNA3.1 plasmids and the D399S/M686V/I687A-$GluR1_i$-pGEMHE-3Z plasmid were constructed using the QuikChange mutagenesis kit according to the manufacturer's instructions (Stratagene, La Jolla, CA). The absence of unwanted mutations was verified by sequencing the cDNAs of all mutant GluRs.

Cell Culture of Stable GluR-HEK293 Cell Lines. HEK293 cell lines stably expressing $GluR1_i$, $GluR2Q_i$, $GluR3_i$, and $GluR4_i$ were maintained at 37 °C in a humidified 5% CO_2 incubator in Dulbecco's modified Eagle medium (DMEM) supplemented with penicillin (100 U/mL), streptomycin (100 μg/mL), G-418 (1 mg/mL), and 5% dialyzed fetal bovine serum (in the case of the $GluR3_i$ cell line, 10% dialyzed fetal bovine serum).

Generation and Cell Culture of Polyclonal GluR-HEK293 Cells. The HEK293 cells used generating polyclonal cells expressing wild type (WT) and mutant GluRs were maintained in DMEM

supplemented with penicillin (100 U/mL), streptomycin (100 μg/mL), and 5% dialyzed fetal bovine serum. The cells were transfected with the WT $GluR1_i$-pcDNA3.1, WT $GluR4_i$-pcDNA3.1, and mutant $GluR1_i$-pcDNA3.1 plasmids using Polyfect as a DNA carrier according to the protocol of the manufacturer (Qiagen, Hilden, Germany). The transfected cells were maintained for 2−3 weeks in selection medium containing 3 mg/mL G-418 before the functional properties of the respective receptors were characterized in the Fluo-4/Ca^{2+} assay described below.

The Fluo-4/Ca^{2+} Assay. The functional properties of the Tet-AMPA analogues were characterized at the stable $GluR1_i$-, $GluR2Q_i$-, $GluR3_i$-, and $GluR4_i$-HEK293 cell lines and at the polyclonal HEK293 cells expressing WT and mutant GluRs in the Fluo-4/Ca^{2+} assay as previously described.[15] The stable (monoclonal) and polyclonal HEK293 cells were split into poly-D-lysine-coated black 96-well plates with clear bottom (BD Biosciences, Bedford, MA). Later (16−24 h) the medium was aspirated, and the cells were incubated in 50 μL of loading buffer [Hank's buffered saline solution (HBSS) containing 20 mM HEPES, 1 mM $CaCl_2$, 1 mM $MgCl_2$, and 2.5 mM probenecid, pH 7.4] supplemented with 6 mM Fluo4/AM (Molecular Probes, Eugene, OR) at 37 °C for 1 h. The loading buffer was aspirated, the cells were washed with 100 μL loading buffer, and then 100 μL assay buffer [HBSS supplemented with 20 mM HEPES, 10 mM $CaCl_2$, 1 mM $MgCl_2$, 2.5 mM probenecid and 100 μM CTZ, pH 7.4] was added to the wells. Then the 96-well plate was assayed in a NOVOstar microplate reader (BMG Labtechnologies, Offenburg, Germany) measuring emission [in fluorescence units (FU)] at 520 nm caused by excitation at 485 nm before and up to 60 s after addition of 33 μL agonist solution (the agonists were dissolved in assay buffer). The compounds were characterized in duplicate or triplicate (i.e., two or three data points for each concentration) at least three times (i.e., at least three different cell passages) at the WT or mutant GluRs. Due to limited quantities of the 2-Bn-Tet-AMPA sample, the compound was tested at a maximal assay concentration of 3 mM.

Electrophysiological Recordings in *Xenopus* Oocytes. Oocytes were isolated and prepared as previously described.[16] cRNA was transcribed using the mMESSAGE mMACHINE T7 kit from Ambion (Austin, TX). In the experiments we used low-Ca^{2+} Ringer's (115 mM NaCl, 0.1 mM $CaCl_2$, 2.5 mM KCl, 1.8 mM MgCl, 10 mM HEPES, pH 7.5) to prevent Ca^{2+}-induced Cl^- currents. Recordings were performed 2−3 days after injection, using a two-electrode voltage clamp. Dose−response curves were constructed by fitting current peak amplitude values obtained at different concentrations in the presence of 100 μM CTZ, after normalization to a 1000 μM glutamate and 100 μM CTZ peak response. A previously described protocol was followed for standard cell treatment with CTZ to obtain maximum efficacy of CTZ on $GluR1_i$ and $GluR4_i$.[17] The nonlinear fitting routine was performed using GraphPad Prism version 4.00. The data was fitted to the Hill equation, $I = 1/[1 + (EC_{50})/[A]^{n_H}]$, where I is the normalized current amplitude induced by the agonist at concentration [A], n_H is the Hill coefficient, and EC_{50} is the concentration at which a half-maximal response was induced.

Molecular Modeling. Homology models were built from the experimental GluR2-S1S2J:(*S*)-2-Bn-Tet-AMPA structure[11] for the hypothetical constructs corresponding to the ligand binding domain S1S2J for WT GluR1−GluR4 and GluR1 mutants D399S, E683A, M686V, I687A, D399S/E683A, M686V/I687A, D399S/M686V/I687A, E683A/M686V/I687A, and D399S/E683A/M686V/I687A, by comparative modeling and side chain refinement in Prime 1.5.[18] Redocking of (*S*)-2-Bn-Tet-AMPA was performed in Glide 4.0[18] using the Extra Precision scoring function.[19] For each resulting complex, the binding energies were estimated by the MM-GBSA approximation[20] implemented in Prime 1.5.[18] Default settings and the vendor's recommended protocols were used throughout.

Acknowledgment. This work was supported by the Lundbeck Foundation and the Danish Medical Research Council.

References

(1) Bräuner-Osborne, H.; Egebjerg, J.; Nielsen, E. Ø.; Madsen, U.; Krogsgaard-Larsen, P. Ligands for glutamate receptors: Design and therapeutic prospects. *J. Med. Chem.* **2000**, *43*, 2609−2645.
(2) Dingledine, R.; Borges, K.; Bowie, D.; Traynelis, S. F. The glutamate receptor ion channels. *Pharmacol. Rev.* **1999**, *51*, 7−61.
(3) Riedel, G.; Platt, B.; Micheau, J. Glutamate receptor function in learning and memory. *Behav. Brain Res.* **2003**, *140*, 1−47.
(4) Javitt, D. C. Glutamate as a therapeutic target in psychiatric disorders. *Mol. Psychiatry* **2004**, *9*, 984−997.
(5) Jensen, A. A. Molecular pharmacology of the metabotropic glutamate receptors. In *Molecular Neuropharmacology. Strategies and Methods*; Schousboe, A., Bräuner-Osborne, H., Eds.; Humana Press: Totowa, NJ, 2004; pp 47−82.
(6) Mayer, M. L.; Armstrong, N. Structure and function of glutamate receptor ion channels. *Annu. Rev. Physiol.* **2004**, *66*, 161−81.
(7) Bjerrum, E. J.; Kristensen, A. S.; Pickering, D. S.; Greenwood, J. R.; Nielsen, B.; Liljefors, T.; Schousboe, A.; Bräuner-Osborne, H.; Madsen, U. Design, synthesis, and pharmacology of a highly subtype-selective GluR1/2 agonist, (*RS*)-2-amino-3-(4-chloro-3-hydroxy-5-isoxazolyl)propionic acid (Cl-HIBO). *J. Med. Chem.* **2003**, *46*, 2246−2249.
(8) Greenwood, J. R.; Mewett, K. N.; Allan, R. D.; Martin, B. O.; Pickering, D. S. 3-hydroxypyridazine 1-oxides as carboxylate bioisosteres: A new series of subtype-selective AMPA receptor agonists. *Neuropharmacology* **2006**, *51*, 52−59.
(9) Frandsen, A.; Pickering, D. S.; Vestergaard, B.; Kasper, C.; Nielsen, B. B.; Greenwood, J. R.; Campiani, G.; Fattorusso, C.; Gajhede, M.; Schousboe, A.; Kastrup, J. S. Tyr^{702} is an important determinant of agonist binding and domain closure of the ligand-binding core of GluR2. *Mol. Pharmacol.* **2005**, *67*, 703−13.
(10) Vogensen, S. B.; Clausen, R. P.; Greenwood, J. R.; Johansen, T. N.; Pickering, D. S.; Nielsen, B.; Ebert, B.; Krogsgaard-Larsen, P. Convergent synthesis and pharmacology of substituted tetrazolyl-2-amino-3-(3-hydroxy-5-methyl-4-isoxazolyl)propionic acid analogues. *J. Med. Chem.* **2005**, *48*, 3438−42.
(11) Vogensen, S. B.; Frydenvang, K.; Greenwood, J. R.; Postorino, G.; Nielsen, B.; Pickering, D. S.; Ebert, B.; Bølcho, U.; Egebjerg, J.; Gajhede, M.; Kastrup, J. S.; Johansen, T. N.; Clausen, R. P.; Krogsgaard-Larsen, P. A tetrazolyl substituted subtype-selective AMPA receptor agonist. *J. Med. Chem.* **2007**, *50*, 2408−14.
(12) Bang-Andersen, B.; Lenz, S. M.; Skjærbæk, N.; Søby, K. K.; Hansen, H. O.; Ebert, B.; Bøgesø, K. P.; Krogsgaard-Larsen, P. Heteroaryl analogues of AMPA. Synthesis and quantitative structure−activity relationships. *J. Med. Chem.* **1997**, *40*, 2831−42.
(13) Vogensen, S. B.; Jensen, H. S.; Stensbøl, T. B.; Frydenvang, K.; Bang-Andersen, B.; Johansen, T. N.; Egebjerg, J.; Krogsgaard-Larsen, P. Resolution, configurational assignment, and enantiopharmacology of 2-amino-3-[3-hydroxy-5-(2-methyl-2*H*-tetrazol-5-yl)isoxazol-4-yl]-propionic acid, a potent GluR3- and GluR4-preferring AMPA receptor agonist. *Chirality* **2000**, *12*, 705−13.
(14) Hogner, A.; Kastrup, J. S.; Jin, R.; Liljefors, T.; Mayer, M. L.; Egebjerg, J.; Larsen, I. K.; Gouaux, E. Structural basis for AMPA receptor activation and ligand selectivity: Crystal structures of five agonist complexes with the GluR2 ligand-binding core. *J. Mol. Biol.* **2002**, *322*, 93−109.
(15) Strange, M.; Bräuner-Osborne, H.; Jensen, A. A. Functional characterisation of homomeric ionotropic glutamate receptors GluR1-GluR6 in a fluorescence-based high throughput screening assay. *Comb. Chem. High Throughput Screen.* **2006**, *9*, 147−158.
(16) Nielsen, M. M.; Liljefors, T.; Krogsgaard-Larsen, P.; Egebjerg, J. The selective activation of the glutamate receptor GluR5 by ATPA is controlled by serine 741. *Mol. Pharmacol.* **2003**, *63*, 19−25.
(17) Fucile, S.; Miledi, R.; Eusebi, F. Effects of cyclothiazide on GluR1/AMPA receptors. *Proc. Natl. Acad. Sci. U.S.A.* **2006**, *103*, 2943−7.
(18) Prime 1.5, Glide 4.0; Schrödinger Inc., S. M. S.: Portland, OR, 2006.
(19) Friesner, R. A.; Murphy, R. B.; Repasky, M. P.; Frye, L. L.; Greenwood, J. R.; Halgren, T. A.; Sanschagrin, P. C.; Mainz, D. T. Extra precision glide: Docking and scoring incorporating a model of hydrophobic enclosure for protein-ligand complexes. *J. Med. Chem.* **2006**, *49*, 6177−96.
(20) Yu, Z.; Jacobson, M. P.; Friesner, R. A. What role do surfaces play in GB models? A new-generation of surface-generalized born model based on a novel Gaussian surface for biomolecules. *J. Comput. Chem.* **2006**, *27*, 72−89.

JM070532R